THE FAST EJECTION SYSTEM OF THE CERN 25 GeV PROTON SYNCHROTRON

R. Bertolotto, H. van Breugel, L. Caris, E. Consigny, H. Hijkhuisen, J. Goni, J. J. Hirsbrunner, B. Kuiper, S. Milner, S. Pichler, G. Plass

CERN

(Presented by B. KUIPER)

1. INTRODUCTION

In view of the probable need for high intensity beams, small angle production of secondaries and beams of short lived particles, it was, after the completion of the CPS, on general grounds decided to build ejection equipment covering as many of the foreseeable applications as possible. The applications seemed essentially to be composed of two classes. On one hand, groups specialized in counter experiments were interested in beams extending as far as possible in time, e. g. some hundreds of milliseconds. For bubble chamber experiments, on the other hand, bursts of 100 μs or less are convenient. In some applications, such as in emulsion experiments, there did not seem to be much preference. Though not essential in several of the cases, high efficiency and «cleanness», i. e. low contamination of the exracted protons by secondary particles, seemed generally desirable features. This also, because of the habit of deflected but not ejected protons to create spurious background in not entirely predictable places and high activity of equipment needing routine maintenance.

Some prelimenary studies had then already been made by Citron [1]. However, considering the characteristics of the CPS, it became clear that the long revolution time of 2 μs could yield the possibility for entirely electro-magnetic ejection in times of the order of one revolution [2]. The low circumferential filling factor of protons in the machine stimulated the idea to combine very high efficiency with extreme cleanness. Some trajectories revealed the possibility of very low extracted beam emittances. Though such a «fast ejection» would only cover part of the applications, work on it started first due to above attractive and challenging features. Work on «slow ejection» also followed by Krienen [3] and later by Hereward [4] and some hardware is now approaching its completion, but this will not be part of this paper.
In the meantime the CERN radio frequent separator, now under construction, had been based on fast beam deflection and, for later stages, the use of a fast extracted beam had been planned. Finally, the enhanced neutrino experiment, preparations for which were gradually gathering momentum in CERN, in addition to its need for a high flux, proposed to use the low duty cycle to gate against cosmic ray background. It is in this experiment, presently being carried out at CERN, that the fast ejection system has become a necessary condition for success.

All extraction schemes have in common the use of an ejection field (shimming of the main field, perturbation thereof, separate magnet, etc.), i. e. a localized field pattern that makes the particles diverge out of the stable region of the guiding-field whenever the beam is perturbed more than some limiting value from its closed equilibrium orbit. The difference between fast, slow or intermediate systems is then given by the respective times taken to subsequently perturbing all particles from their stable orbit. The build-up time of the radial excursion of the particles after the onset of the perturbation is not relevant for fast or slow but generally governs the efficiency of the scheme as follows. The limiting value of the perturbation can never be a rigorous discontinuity but rather there exists a transition region of the field to which corresponds a range of perturbations resulting neither in ejection nor in focusing back of the particles towards the closed equilibrium orbit. The particles in question are usually lost against the vacuum chamber of the accelerator or against other hardware. If it is possible to create a perturbation which

builds up the radial excursion of the particles so rapidly that their trajectory is stable in one revolution but enters the diverging field region in the subsequent one, in other words, if one can make the particle jump the transition region from one revolution to the next, it is possible to obtain close to 100% extraction efficiency, provided the onset of the radial excursion is always on the same place along the circumference of the accelerator.

In the CPS fast ejection system the ejection field is given by a separate magnet, called «bending magnet», located in a long straight section 1, reserved for such applications in the design of the accelerator. An obvious and clean disturbance of the protons is a magnetic field, called «kicker magnet», acting on the beam somewhere upstream, such that the angular deflection created there transforms into a radial displacement of the protons adequate to jump the transition region of the ejection field in the bending magnet. Advantage is taken of the RF structure of the beam to make the perturbating field in the kicker magnet rise to its nominal value between the passage of two subsequent proton bunches. The principal conditions for clean ejection with close to 100% efficiency are thus fulfilled and the entire beam will be ejected in the time of one revolution or 2.1 μs, preserving the RF structure. A concomitant feature is the extremely low duty cycle permitting the hitherto impossible rejection against continuous background radiation of 10^6 to 1 for the beam or 10^7 to 1 for the bunches. The constant and very nearly homogeneous field in the kicker magnet and the bending magnet permits conservation of a beam-emittance close to the one in the accelerator. This is only slightly offset by non-linearities in the strayflux of the CPS magnet.

2. SOME PARAMETERS

Though the characteristics of the CPS have been described before, e. g. by Regenstreif [5], the repetition of some main parameters is here relevant. At the beginning of the CPS acceleration cycle the proton beam is rather diffuse and fills a large part of the elliptical machine aperture of 150 mm wide and 75 mm high. Adiabatic damping of the betatron oscillation makes the beam diameter shrink rapidly during acceleration, such that it is around 12 mm at 10 GeV, 10 mm at 17 GeV and 7 mm at 25 GeV. Hence, for all practical applications close to 100% of the beam current is within a circular cross section of 10 mm ∅, apart from a diffuse halo around the beam, continuously being created by scattering with the residual gas. Radial position instabilities in one cycle and from pulse are from a few tenths to 1 or 2 mm, depending on energy and machine condition. The vertical stability is better. In the second part of the accelerator cycle closed orbit distortions, both vertical and horizontal, are of the order of a few mm.

The number of betatron oscillations on the circumference of the CPS of around 6.25 together with the ring-diameter of 200 m results in a wavelength of 100 m. At relativistic energies the 10 MHz accelerating frequency yields a spacing of the proton bunches in time of 105 ns. For the given machine diameter the circumference of the accelerator then contains 20 bunches and the revolution time of the protons is 2.1 μs. Damping of the synchrotron oscillations brings the bunch length down to less than 10 ns in time, before the time relevant for ejection.

Engineering considerations, such as minimization of angular deflections and of energies and voltages, led to a decision for small magnet apertures, enough to contain the beam and allowing for position incertainties and adequate clearings. It then becomes necessary to use the septum construction for the bending magnet, thus minimizing the transition region, and to operate it as close to the undisturbed orbit as beam-instabilities and the leakage field of the bending magnet will allow. Since by their small gaps the kicker magnet and bending magnet must during operation block a part of the useful aperture of the accelerator, these magnets must be brought into their working position in the second half of the acceleration cycle when the beam has shrunk to the quoted dimensions. The machine aperture is thus left unobstructed right after injection when its full section is needed. The cited beam diameter, a reasonable clearance between beam and magnet poles of a few mm and the usual departure from homogeneity of the field close to the outside of the gap of C-shaped magnets give 15 mm high and 25 mm wide as convenient dimensions for the KM aperture. The available space between two magnet units in the short straight section 97 limits the total length of the kicker magnet to 0.90 m.

Similar considerations hold for the bending magnet but some more horizontal space is provided to allow for variations in horizontal

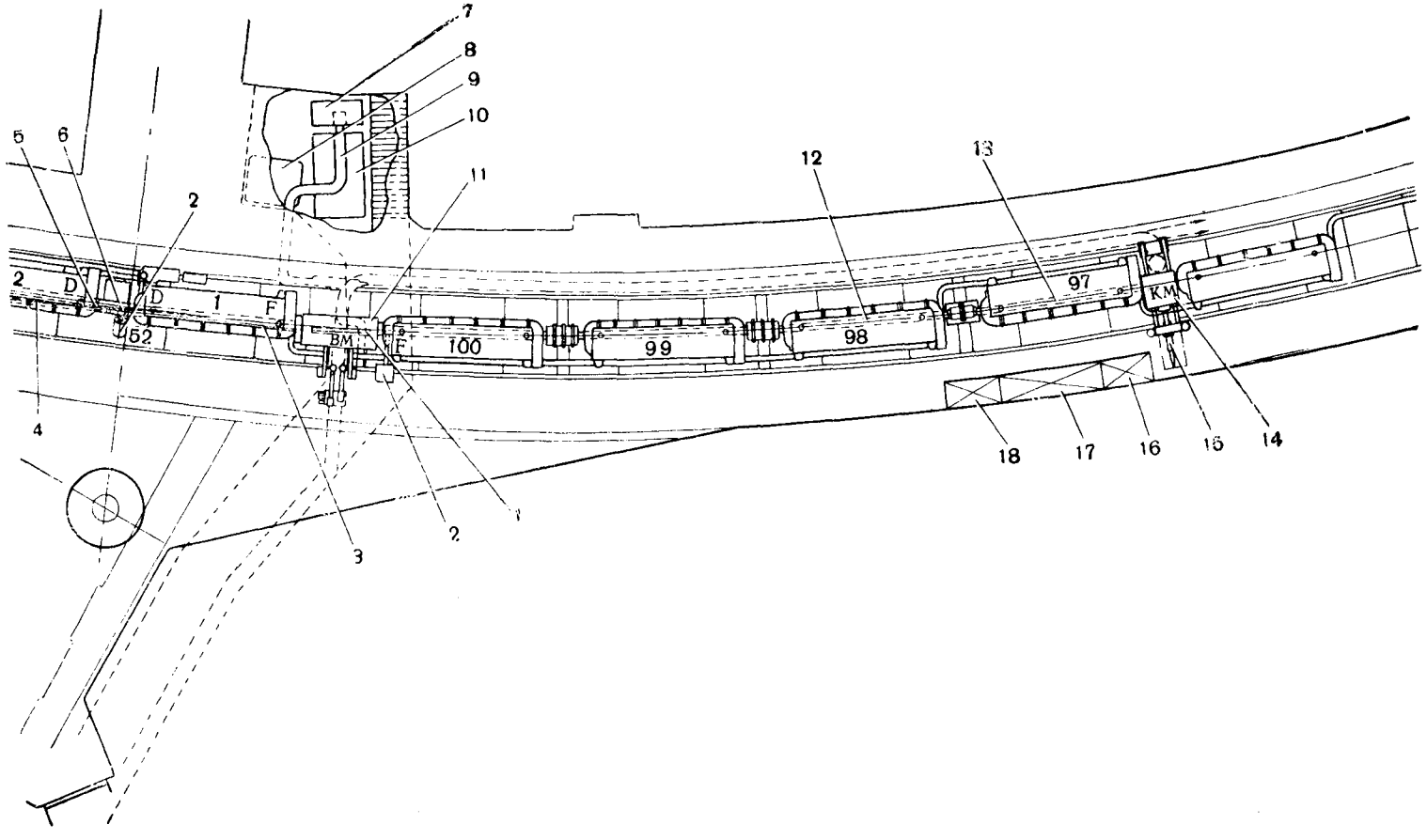

Fig. 1. Layout of the fast ejection system:

1 — fluorescent frame around aperture on end of bending magnet; *2* — screened TV camera; *3* — ejected beam; *4* —vacuum pipe; *5* — current transformer for ejected beam; *6* — fluorescent screen for extracted beam; *7* — ignitron rack; *8* — heat exchanger, *9* — low inductance parallel plate conductor to BM; *10* — capacitor bank; *11* — special tank SS1 for fast ejection bending magnet; *12* — vacuum chamber of CPS; *13* — equilibrium orbit; *14* — special tank SS97 for kicker magnet; *15* — hydraulic actuator; *16* — terminating resistors; *17* — pulse generator and trigger; *18* — control cubicle HV set.

beam displacement due to possible inconstancy of the kick, small vertical displacements due to a possible radial component in the KM field and for the curvature of the trajectory in the bending magnet, which consists of two straight halves inclined to each other. The aperture of the BM is then taken 25 mm high and 45 mm wide. The long straight section 1 permits a total length of 2 m. The minimum deflection angle of the BM for ejecting the beam is 16 mrad.

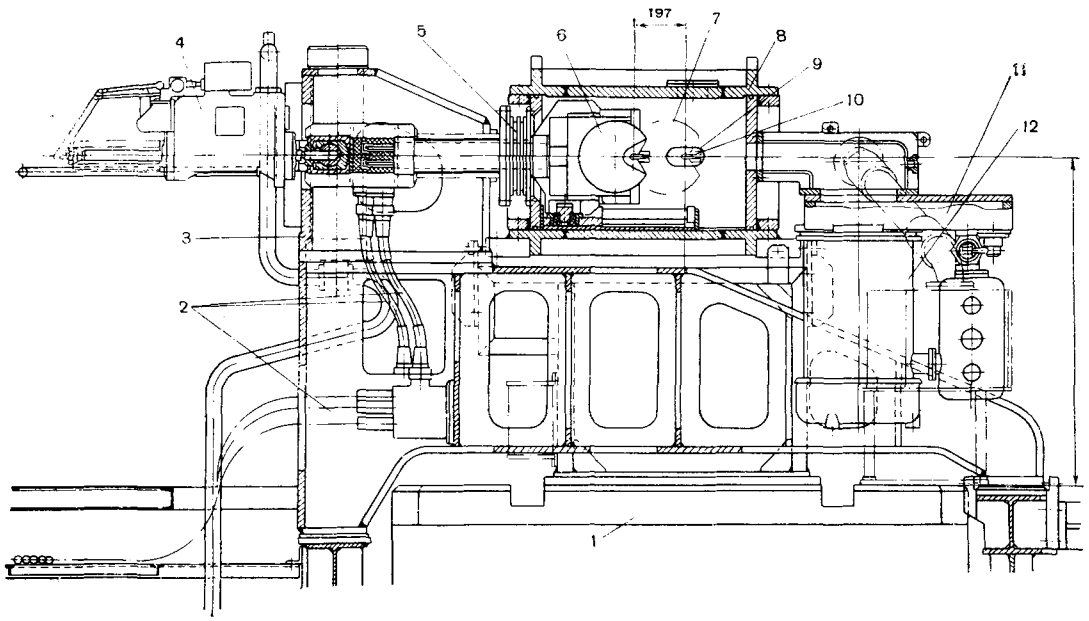

Fig. 2. Sectional view of the kicker magnet in its vacuum tank:
1 — concrete ring beam supporting CPS magnet; *2* — pulse cables; *3* — steel girder supporting actuator; *4* — hydraulic actuator; *5* — vacuum seal; *6* — kicker magnet in rest position; *7* — kicker magnet in working position; *8* — vacuum tank in SS97; *9* — normal machine aperture; *10* — beam; *11* — vacuum valve; *12* — vacuum pump.

At 25 GeV/c proton momentum this corresponds to a field of 0.65 Wb/m² over the length of 2 m. The beam diameter and the chosen septum thickness of 6 mm give with reasonable operating clearance, a required minimum beam displacement of 20 mm for ejection. A convenient operating value is 25 mm. This corresponds to 1.1. mrad of deflection of the kicker magnet for which a field of 0.1 Wb/m² is needed over the length of 0.90 m.

3. LAYOUT AND OUTLINE

Fig 1. shows a layout of the fast ejection system. The bending magnet is in the long straight sectine 1, which is convenient, for the following three CPS magnet units are of the inside type, leaving the space free for the extracted beam. The kicker magnet is one quarter of a betatron wavelength upstream in the short straight section 97. The two magnets are located in the CPS vacuum system which is locally enlarged to boxes that contain the magnets and their displacement. The movement is given by hydraulic actuators outside the vacuum boxes over a connection shaft that slides through a vacuum seal. Fig. 2 and Fig. 3 give sectional views fo respectively the kicker magnet and bendnig magnet in their vacuum tanks. In the first half of CPS magnet unit No 1 the vacuum tube is widened at the exterior to contain the deflected beam. In the centre of this unit it splits in two and a separate, narrow pipe takes the ejected beam out of the machine. The pulse generators are kept close to the magnets. For the kicker magnet it is in the CPS ring, for the bending magnet in the basement. The dc supplies for charging the capacitors and lines are located outside the machine.

Although more than one method is known [2] for obtaining a fast rise followed by a constant field in the kicker magnet during the 2 μs of extraction, the delay line system proposed [6] and first applied [7] by O'Neill was adopted for

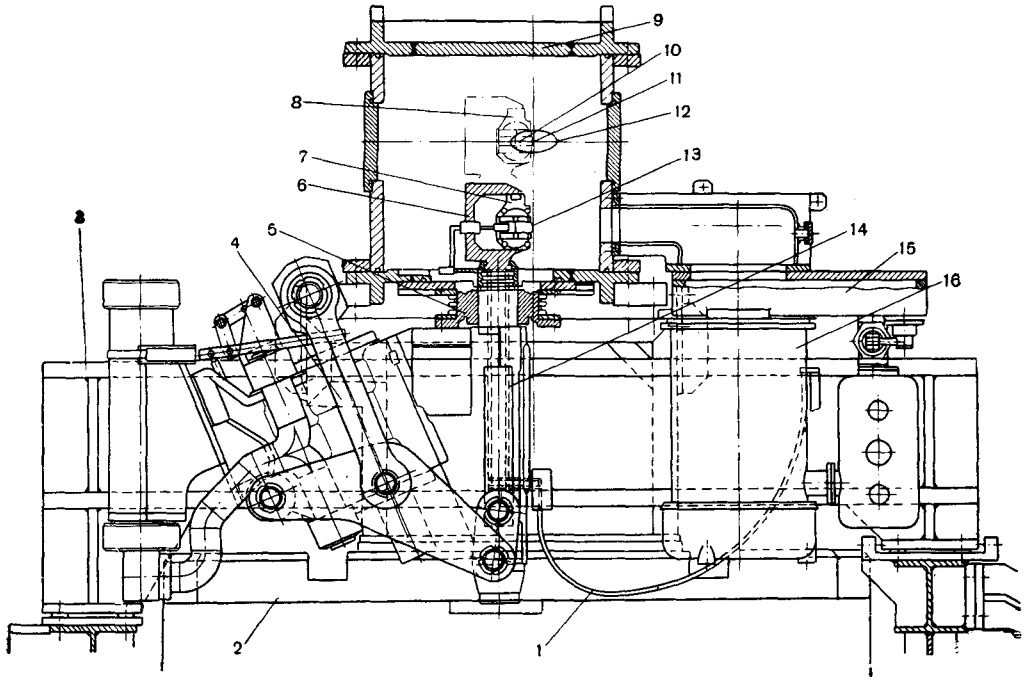

Fig. 3. Sectional view of the bending magnet in its vacuum tank:
1 — flexible low inductance feeds; *2* — concrete ring beam supporting CPS magnet; *3* — steel girder supporting actuator; *4* — hydraulic actuator; *5* — vacuum seal; *6* — supporting beam; *7* — bending magnet in rest position; *8* — bending magnet in working position; *9* — vacuum tank in SSI; *10* — kicked beam; *11* — unperturbed beam; *12* — normal machine aperture; *13* — septum; *14* — coaxial HV traversal; *15* — vacuum valve; *16* — vacuum pump.

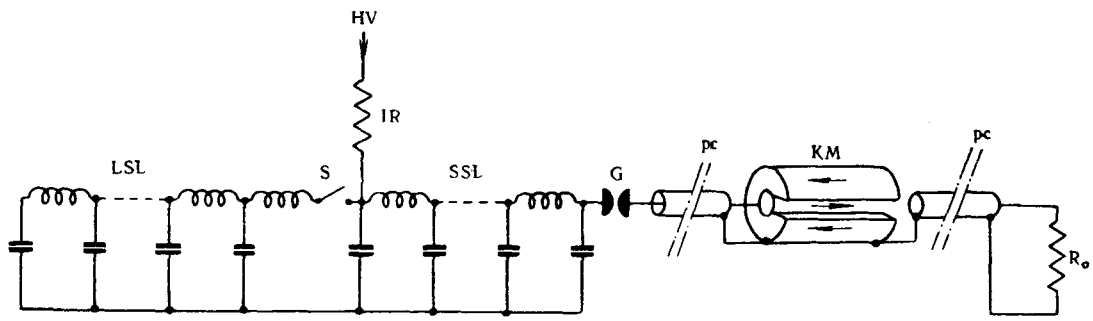

Fig. 4. Principle of the kicker magnet circuit:
HV — charging line from high voltage set; *IR* — isolating resistor; *LSL* — long storage line; *S* — switch (when closed: 2μS pulse, when open: 100 ns pulse); *SSL* — short storage line; *G* — sparkgap; *pc* — pulse cables; *KM* — kicker magnet; R_0 — matched terminating resistors.

its relative simplicity of circuit and switchgear and for its possibility to terminate the pulse. The latter permits partial extraction of the beam, leaving the remainder undisturbed for internal targeting applications or slow ejection. The principle of the kicker magnet circuit is given in Fig. 4. All parts of the circuit are matched to the impedance of 10 Ω. The kicker magnet is a fourpole and has delay line characteristics. Two pulse forming networks connected in series by a switch S are charged from a HV power supply through an isolating resistor IR. If the gap G is fired a rectangular pulse of twice the delay time of the lines and half the charging

voltage propagates to the right, traverses the kicker magnet and is dissipated in the terminating resistors.

The bending magnet field has the requirement of low leakage fields, met by the septum construction, and high constancy of the field during the 2 μs of passage of the kicked beam. To reduce cooling requirements and the leakage field this magnet is also pulsed, for simplicity with a half sine wave of ~ 150 μs base. The pulse is derived from a crowbar circuit according to Fig. 5. When the capacitor bank is switched

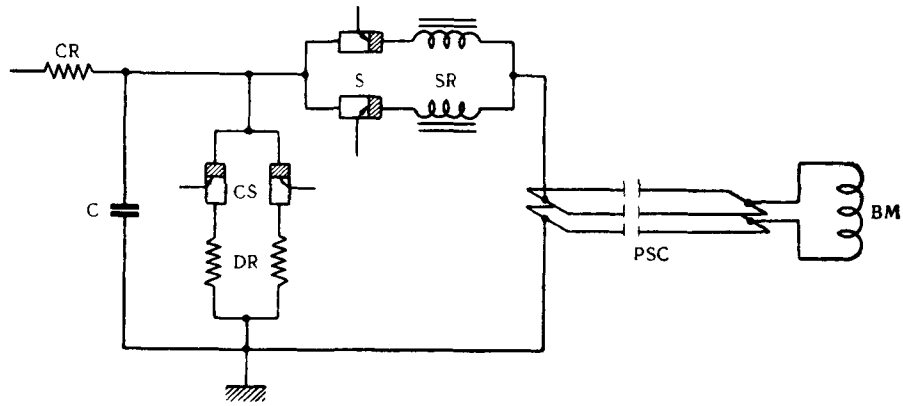

Fig. 5. Principle of bending magnet circuit:
CR — charging resistor; *C* — capacitor bank; *S* — switching ignitrons; *SR* — saturable reactors; *CS* — crowbar switch; *DR* — dumping resistors; *PSC* — parallel strip conductors; *BM* — bending magnet.

to the inductance of the magnet excitation loop, the circuit starts a ringing discharge. After the first half wave, when the capacitor voltage is reversed and the current is zero, the crowbar switch CS shunts the coil with a resistor R. The saturable reactors having permitted the gap S to extinguish the capacitor bank will dissipate its energy in the resistor in a single, damped current surge. The 2 μs KM pulse is synchronized on the crest of the BM pulse.

4. THE KICKER MAGNET AND ITS CIRCUIT

The theory of the delay line magnets has been treated in detail elsewhere [2, 6, 8]. Here it is useful to elucidate the coherence of the parameters by the following argument. The available length l and the chosen width b of the aperture and height h determine the inductance of the kicker magnet with single loop excitation by

$$L_k \approx \mu_0 \frac{l \cdot b}{h}. \qquad (1)$$

The magnetic kick K, defined as

$$K = \int_0^l B\,dS, \qquad (2)$$

where B is the magnetic field in the kicker, and S the coordinate along the trajectory, is subject to requirements for magnitude and risetime. The latter is for a delay line magnet, essentially its delay time T_k, provided the leading edge of the current pulse is considerably shorter. This determines the capacity C_k of the kicker magnet by

$$T_k \approx \sqrt{L_k \cdot C_k} \qquad (3)$$

and hence the impedance Z as

$$Z = \sqrt{L_k / C_k}. \qquad (4)$$

The gap height h and the required angular deflection, hence kick, gave the current i

$$i = \frac{B \cdot h}{\mu_0} \qquad (5)$$

and the voltage V_k

$$V_k = i \cdot Z = \frac{K \cdot b}{T_k} \qquad (6)$$

the charging voltage V_L of the line being twice this value.

In order to keep this voltage limited one will, according to (6), take the maximum delay time for the kicker that is compatible with the requirement of rise time, leaving some margin for jitter in synchronization and non-zero rise time of the current pulse. The impedance can most

conveniently be chosen to fit some nearby combination of standard resistors or transmission cables. If the voltage is still to be reduced the only way is division of the kicker magnet into units, in case the total length is given, or, if space is available, the addition of kicker magnets using a fraction of the current in each. In both ways the voltage is reduced by a corresponding factor. For the CPS a division into two units yielded acceptable voltages. Each unit is excited by its own pulser, permitting their separate use. The main parameters of the kicker magnet circuit are collected in Table 1.

Table 1

Parameters of kicker magnet circuit (per unit)

Number of units	2
Gap height /Ferrite	22 mm
Gap height \Useful for beam	15 mm
Gap width /Ferrite	32 mm
Gap width \Useful for beam	25 mm
Length	450 mm
Ferrite length	280 mm
Pulse duration	2.1 μs 0.10 μs*
Delay time kicker	~0.07 μs
Inductance of kicker	~0.7 μH
Capacitance of kicker	~6600 pF
Characteristic impedance	~10.4 Ω
Max. kicker voltage**	35 kV
» line voltage	70 kV
» current	3500 A
» energy in storage line	260 J 13 J*
» magnetic energy in kicker	9.3 J
» electrostatic energy in kicker	9.3 J
» obtainable kick in entire magnet	0.153 Wb/m
Max. field in Ferrite	~0.3 Wb/m²

* value for single bunch ejection;
** maximum means highest value used over at least 10^6 operations.

As for the highest machine energies and for the envisaged maximum deflection line voltages well above 50 kV were expected, special attention was given to the high voltage engineering. At these voltages pulsed devices using open insulators, e. g. open ends etc., suffer from severe problems of surface flash-over. For this reason, for purposes of matching and to reduce interference production an entirely coaxial construction was adopted. Fig. 6 shows the two pulse generators with their triggering gear and controls.

The box on top of the rack is a 20 section lumped element delay line (long storage line or LSL) giving a pulse of 2.1 μs flat top, the cylinder halfway the column is a 9 section lumped element line (short storage line or SSL), producing a 0.1 μs pulse. Between them is the coaxial switch (S in Fig. 4), operated by oil pressure, and below the short storage line is the triggered sparkgap. When the latter is fired the pulse traverses a tube containing pulse observation probes and is transmitted towards

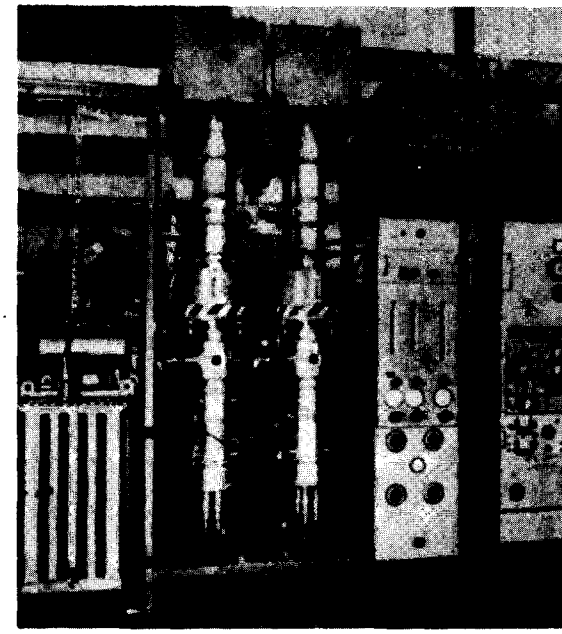

Fig. 6. Pulse generators for the kicker magnet. Center: Two coaxial lines with sparkgaps. Left: High voltage set. Right top: High voltage distribution box. Lower right side: Triggering gear and local controls.

the kicker magnet through 5 BICC type 100 P4 pulse cables of 50 Ω in parallel. The elements of the pulsers are connected to each other with biconical plugs with silicon HV grease, as can be seen in Fig. 7 giving the construction of the sparkgap. The resulting magnetic pulse in the kicker magnet is shown in Fig. 21.

This gap is of the three electrode swinging cascade type described by Fitch and McCormick [9] and can be operated at different voltages by changing its air pressure. The centre electrode is kept on half the (negative) charging voltage of the main electrodes by a high impedance voltage divider. The positive triggering pulse almost immediately breaks down the 0.5 mm gap between the sharp triggering needle and the centre electrode, ionizing upper and

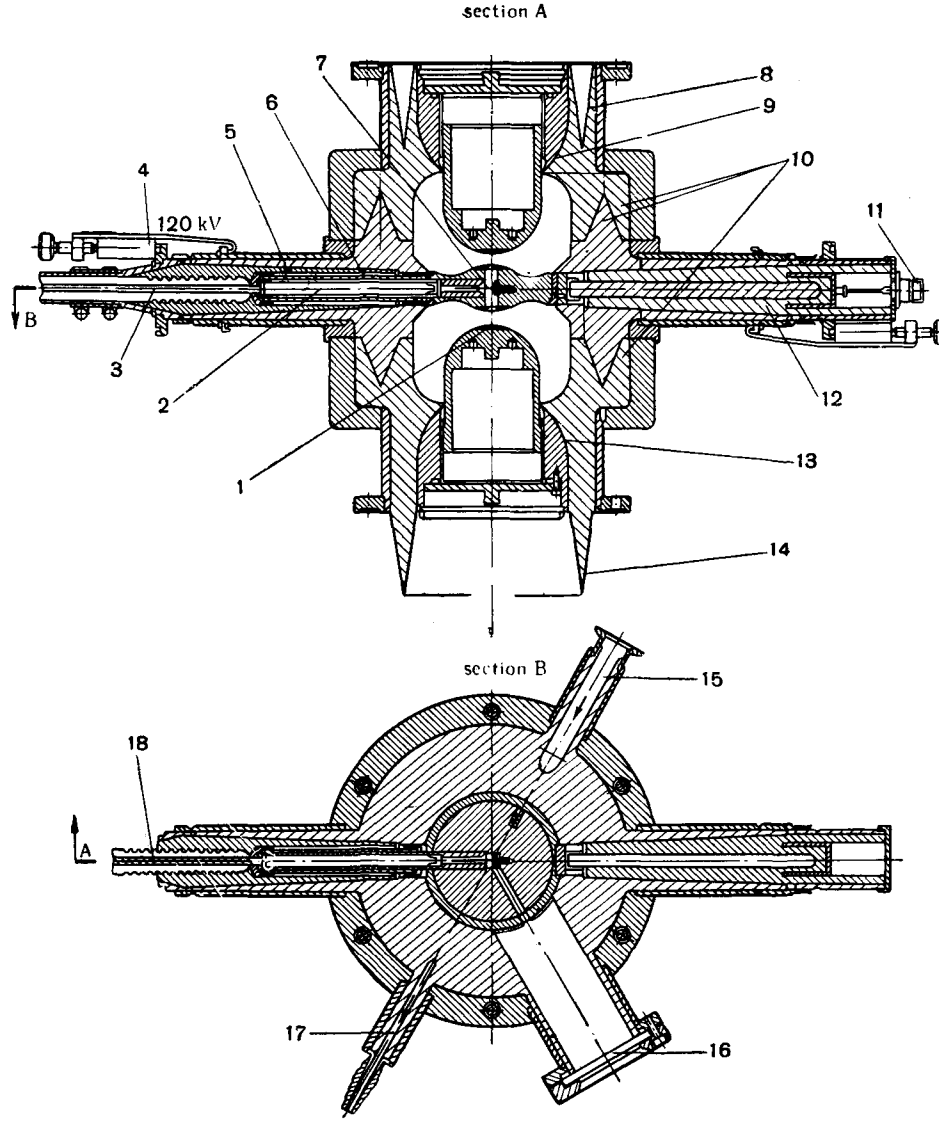

Fig. 7. Coaxial sparkgap:
1 — tungsten; *2* — 1000 Ω stop resistor; *3* — intermediate dc voltage from divider with superimposed trigger pulse; *4* — spring loading of connector; *5* — teflon insulating tube; *6* — 1 MΩ resistor establishing dc voltage on center electrode; *7* — triggering needle; *8* — biconical connector; *9* — high voltage electrode connected to storage lines; *10* — epoxy resin dielectric; *11* — to measuring cable; *12* — plug containing capacitive voltage pick-up; *13* — low potential electrode connected to kicker magnet; *14* — biconical connector (to be mounted with silicon HV grease); *15* — air inlet from pressure source; *16* — window permitting view of trigger and main discharge; *17* — air outlet to bleeding valve; *18* — dc voltage for center electrode and trigger pulse.

lower gap by ultra-violet irradiation through the holes in the electrode and, in charging the latter, creates a rapid rise of its voltage. The upper gap will fire bringing the full charging voltage over the lower gap, which then also breaks down. The centre electrode then takes the pulse voltage, which is equal to the initial dc level, until the end of the pulse when it is discharged completely and goes up to zero. The gaps of the two lines are triggered simultaneously by a master gap, which in its turn is fired by a hydrogen thyratron. The absolute overall time jitter and the mutual jitter between the two main gaps is of the order of 10 ns.

Each of the two kicker magnet units is essentially made of two coaxial conducting tubes

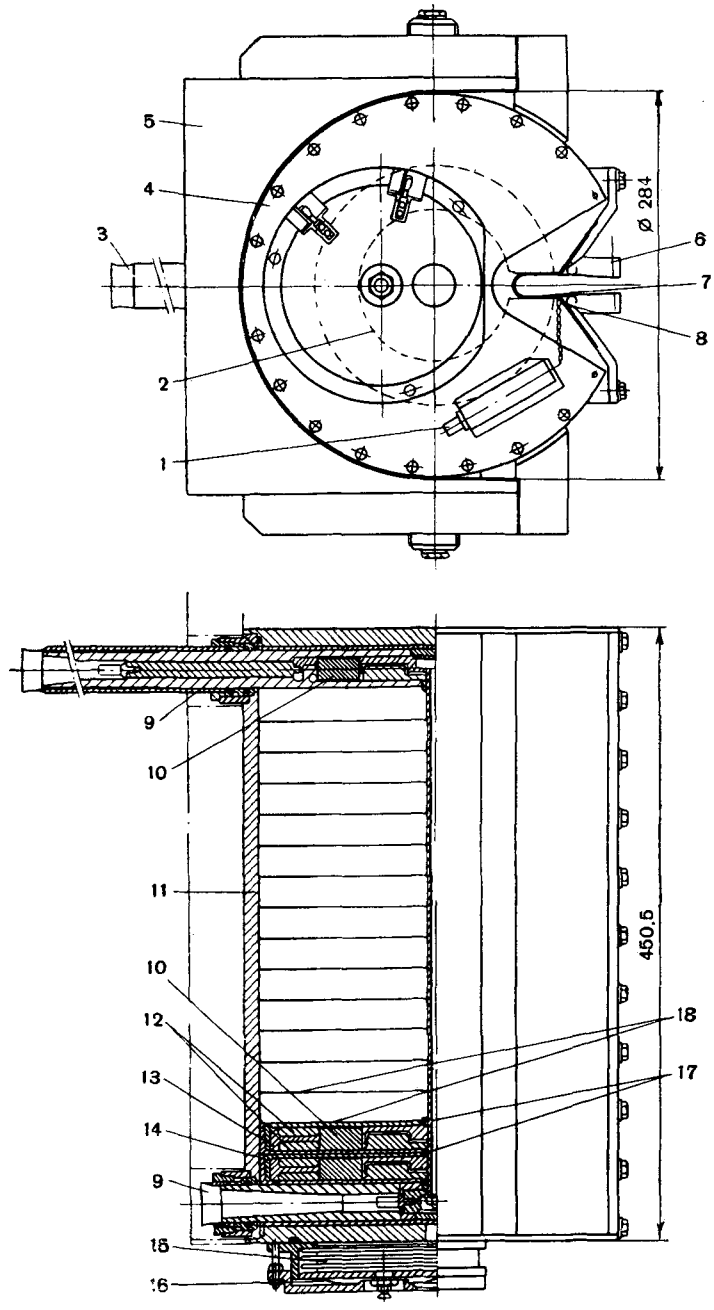

Fig. 8. Structure of the kicker magnet. Top: View on one end of the assembled magnet. Bottom: Horizontal section of one unit: *1* — connector for coaxial measuring cable; *2* — contours of ferrite ring; *3* — connector; *4* — kicker magnet unit; *5* — supporting beam; *6* — beam «razor»; *7* — non-metallic wall in gap; *8* — coil for observation of magnet field; *9* — coaxial connector; *10* — ferrite ring; *11* — aluminium housing; *12* — aluminium cladding of ferrite rings; *13* — cast epoxy resin; *14* — polyethylene boxes; *15* — expansion bellows; *16* — spring loading; *17* — metal spacers for contact between clad ferrite rings; *18* — capacitor plates.

with seventeen ferrite rings between them. The outer tube and the ferrite are cut for the beam aperture. Fig. 8 gives the configuration. Each of the ferrite rings constitutes an inductance and is clad in aluminium. This shields the ferrite from the electric field and keeps it at the inner conductor potential. The capacitors are formed by aluminium foils in contact with the outer conductor and located between two clad ferrite rings with polyethylene as dielectric (cp. Fig. 9). Each magnet unit is vacuum impregnated with

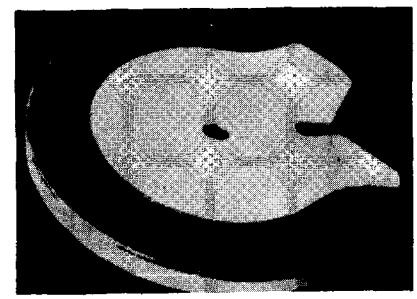

Fig. 9. Assembled kicker magnet section, showing aluminium foil that constitutes a capacity with the inner conductor.

silicon oil and hermetically sealed. The two units are supported together in a C-profiled beam (cf. Fig. 10). Input and output connections go through the transmission shaft linking the magnet in the vacuum to the hydraulic actuator in the air. For constructional reasons these connections had to be mismatched but this has partially been compensated for by capacitors before and after the pieces in question.

After traversal of the kicker magnet the pulse goes again into 5 cables of 50 Ω in parallel, each of them terminated by a 50 Ω resistor in a coaxial configuration with oil dielectric. The 5 resistors are together in an oiltank in which an agitator forces the oil along the resistors and the oil is cooled by a water spiral. The magnetic kick was measured with a single long

loop through the gap of the complete magnet. A zero method was used, balancing the integrated signal against a reference voltage, with an oscilloscope as zero indicator. The setting was better than 1%. Fig. 11 gives the

with the requirement that the field be constant to prescribed accuracy during the 2 μs of ejection. A low duty cycle, i. e. a fast pulse, has the additional advantage that the leakage field can be made small using the eddy current

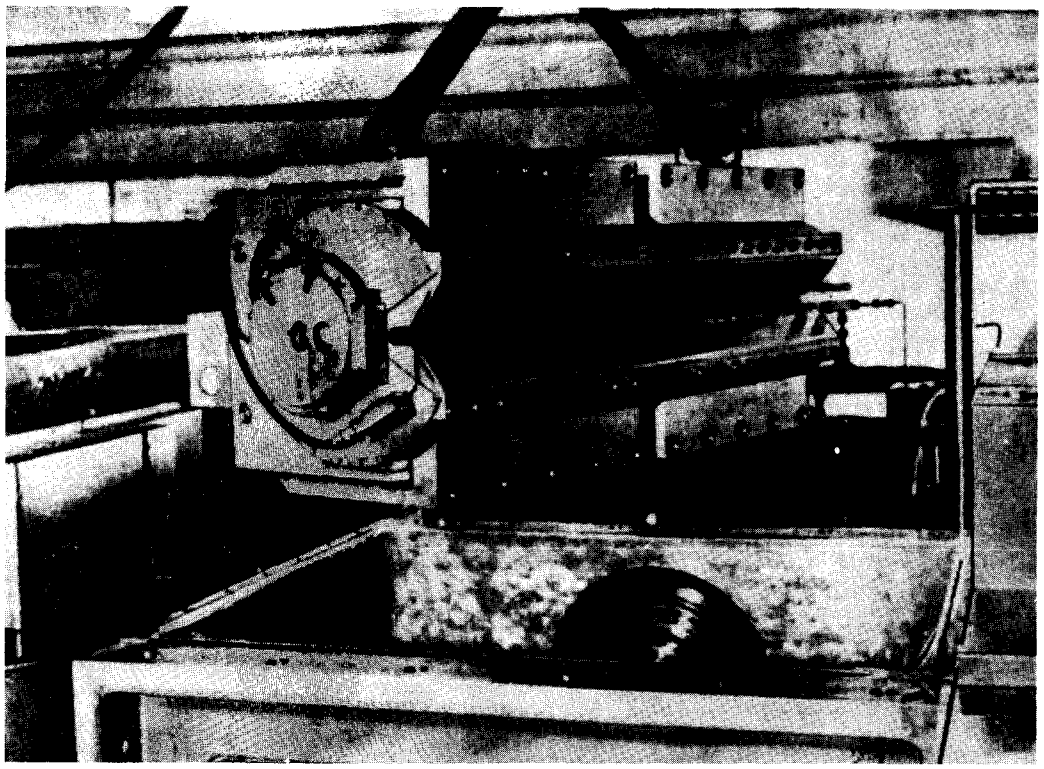

Fig. 10. Assembled kicker magnet above its vacuum tank. Front left: Cable coming from the pulse observation loop in the gap. On the other end of the magnet: The beam-razor fork.

kick as a function of the radial dimension with 60 kV on the line. Fig. 12 shows a magnetization curve combined with a nomogram for finding the beam displacement at the bending magnet. The shape of the curve in Fig. 11 is better than 1% accurate, the levels of Fig. 12 around 5%.

5. THE BENDING MAGNET AND ITS CIRCUIT

For a given nominal current in this magnet the forces due to the field and to thermal stresses are largely a function of the duty cycle. So is the average temperature of the magnet, influencing the dielectric properties of the organic insulation materials. One will hence tend to reduce the duty cycle as much as is compatible

effect, shielding with conducting screens. In order to avoid the complication of pulse-forming networks, a half sinewave pulse was taken. As a normal ringing discharge would dissipate almost the full energy in the magnet excitation loop, a dumping resistor must be incorporated. The present scheme, with the

Table 2

Parameters of the bending magnet circuit

Magnet aperture	45 mm wide 25 mm high
Magnetic length	1.96 m
Inductance of the magnet . .	4.2 μH
Onset of saturation effects . .	around 1.5 Wb/m²
Current at 1.5 Wb/m²	30 kA
Pulser capacitor (HYDRA) . .	328 μF
Capacitor voltage at 1.5 Wb/m²	4.5 kV
Crowbar resistor	0.1 Ω
Crowbar circuit inductance . .	0.2 μH

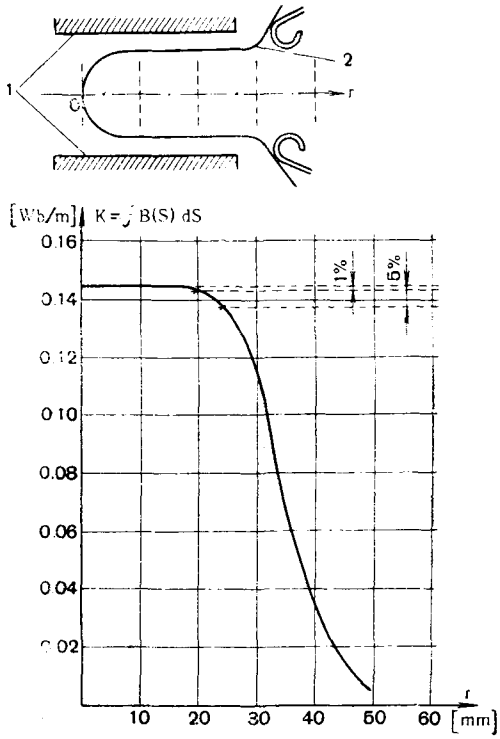

Fig. 11. The kick K as a function of the radial position in the gap of the kicker magnet: *1* — ferrite; *2* — kicker magnet gap.

dumping resistor in the crowbar branch, yields a smaller duty cycle for the magnet than the normal damped series circuit and also requires smaller voltage and energy for a given current. Table 2 gives the parameters of the circuit and Fig. 13 shows an oscillogram of the magnet current and crowbar current.

The main switch S (cp. Fig. 5) and the crowbar switch CS are both composed of two commercial AEI type BK-34 ignitrons in parallel. Each pair of ignitrons is triggered from a hydrogen thyratron, the crowbar switch over an adjustable delay. The low inductance dumping resistor DR consists of folded strips of stainless steel sheet with mylar insulation, clamped between two water cooled plates. For reliable operation and low jitter, which is essential for parallel firing of two ignitrons, the latter are operated at around 25° C. To reduce starting up time a temperature control system first heats the ignitron cooling water, then cools it, as the working temperature is reached. This temperature is kept constant between 24° and 26° C. Fig. 14 shows the bending magnet pulse generator.

The capacitor bank is charged through a Philips type DCG 12/30 thyratron, the grid of which is controlled by the difference between the capacitor voltage and a stabilized preselected reference voltage. Charging is stopped when the reference voltage is reached. This yields a precision of better than 0.4% at 3 kV on the bank. From the capacitor bank and switch gear the pulses are transmitted over low inductance parallel copper strip conductors to the

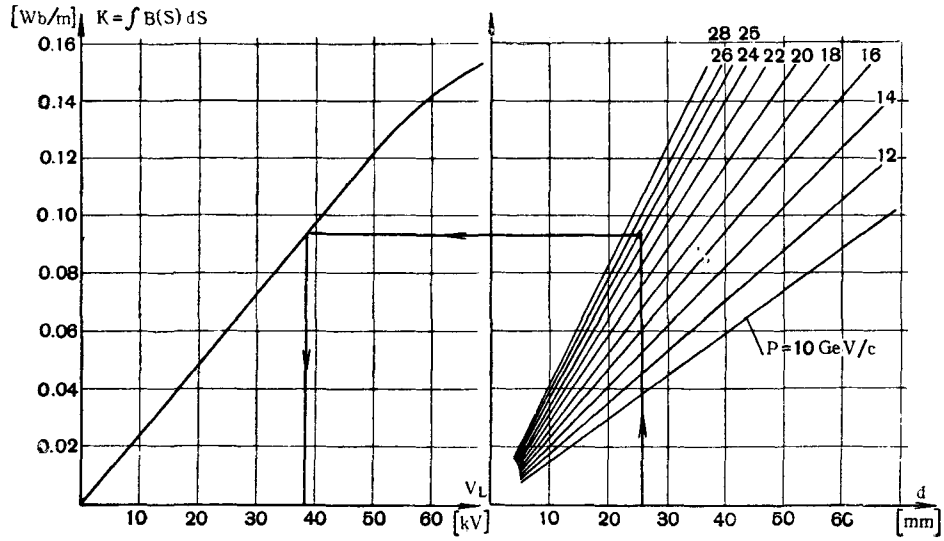

Fig. 12. Magnetization curve of the kicker magnet. Kick K as a function of the line voltage V_L. The nomogram gives the relation between the line voltage, the proton momentum p, and the radial displacement of the beam at the bending magnet.

bending magnet. The flexible leads to the moving magnet are outside the vacuum and the current enters the vacuum box through a coaxial feed in the actuator shaft (cp. Fig. 3).

The bending magnet consists of two straight units of approximately 1 m length supported in a C-profile steel beam which is mounted on the vertical shaft of the hydraulic actuator. The horizontal inclination of the steel beam to

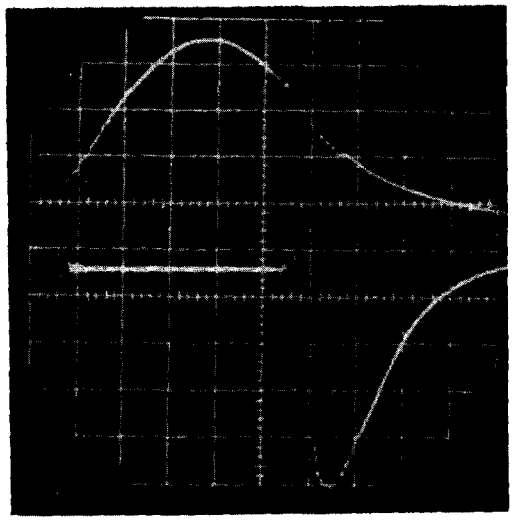

Fig. 13. Top: Bending magnet current. Bottom: Crowbar current.

the equilibrium orbit of the protons in the machine and the angle between the two bending magnet units can be changed to fit different extraction angles and proton energies. Each magnet unit is made of 0.35 mm thick laminations of transformer steel glued together by epoxy resin. The excitation winding is a single loop 2 mm thick copper strip insulated against the magnet iron by layers of mylar sheet to a total of 0.5 mm thick. The leakage field is reduced by use of an eddy current shielding of brass in front of the septum. The shield also gives mechanical support to the latter but increases its total thickness to 6 mm. The septum and the inner conductor are not directly cooled, but transfer their heat to shield, respectively magnet steel which have water pipes fastened to them. Fig. 15 shows the completed structure. The magnetic field in the magnet has been measured point to point by means of Hall probes. Fig. 16 gives the field integrated along the trajectory in the magnet as a function of the radial position, at different excitation levels. Fig. 17 gives a point to point measurement of the leakage field outside the septum along the equilibrium orbit in the machine. Fig. 18 shows this field integrated and expressed as a percentage of the field in the magnet. The homogeneity of the field is

Fig. 14. Bending magnet pulse generator. Front left: Ignitron rack. Behind that: Capacitor bank. Right: Ignition and bending magnet temperature control.

better than 1% for medium fields and better than 2% for saturation fields in the interesting radial range. One can deduce that the kick resulting from the leakage field is always less than 0.015 Wb/m. It occurs only at higher machine energy.

6. CONTROLS AND MONITORING

A block diagram of the controls [10], that coordinate the kicker magnet and bending magnet pulses, the movements of these and the CPS acceleration cycle, is shown in Fig. 19. Apart from the specific controls, such as permitting switching on and off, adjusting voltage or movement, the controls consist mainly, on one

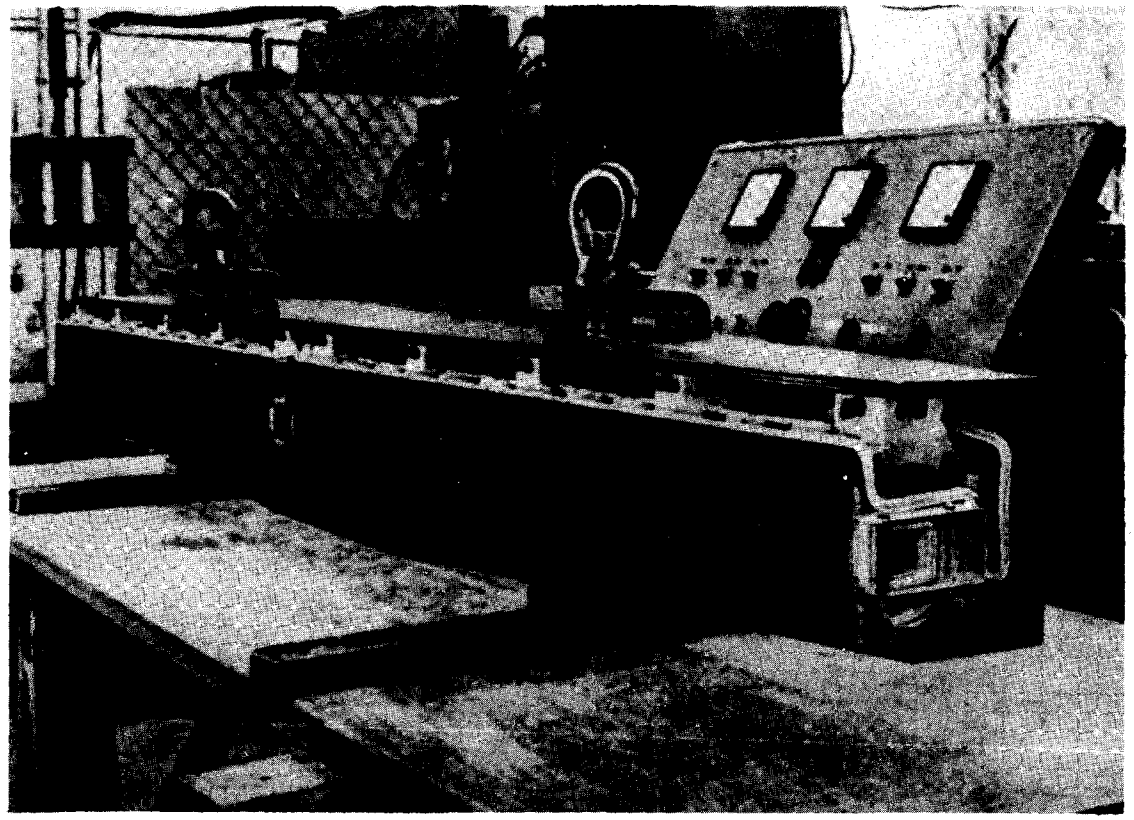

Fig. 15. Assembled bending magnet. Black plate in front is the eddy current shield for reducing the leakage field.

hand, of the so-called fast channel synchronizing kicker magnet with the RF structure of the beam, and on the other hand of the electronic programming system for the hydraulic servo-actuators. The general timing is derived from the so-called M-sequence of pulses, which come at 3.3 ms interval and are synchronous with the CPS acceleration cycle. The ejection and the movement are started by pulses from this sequence, each of the two preselected by means of a separate preset counter timing unit. This permits easy displacement in time of one to another.

Fast channel. Pulses at a repetition frequency of 10 MHz and synchronous with the RF accelerating voltage are frequency divided to give peaked impulses at 2 μs interval. These pass through a gate, a discriminator and a variable delay, then trigger the kicker magnet pulse generators, thus ensuring synchronization between kicker magnet field and RF structure of the beam. The pulse triggering the BM, derived from the M-sequence via one of the two preset counter units gates the RF pulses over a 100 μs variable delay and a gating pulse generator. The moment of ejection is therefore roughly chosen from the M-sequence of the CPS, but the KM is triggered by the first RF pulse passing the gate. The discriminator lets through only healthy unmutilated pulses. The 150 ns variable delay permits adjusting of the rise of the KM field between the bunches.

Programming of the actuators. The hydraulic servo-systems that move the magnets follow an amplitude modulated 400 Hz electric programme voltage, the displacement being proportional to the amplitude of the carrier. The dc programme is first composed in steps by relay units switching at chosen instants to chosen taps of a dc fed potentiometer. It is then smoothed by a filter. The relay units are triggered by 4-coincidence circuits, the instances being chosen by a 4-digit combination on the corresponding cathodes of two 4-place decatron

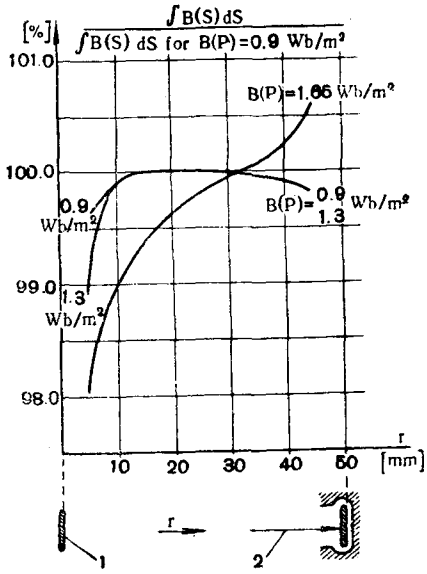

Fig. 16. Integrated field along the bending magnet as a function of the radial position in its gap. Expressed as a percentage of its value at $r = 20$ and at a field $B\ (P) = 0.9$ Wb/m² in the reference point P (cp. sketch of Fig. 18):
1 — septum; *2* — central conductor.

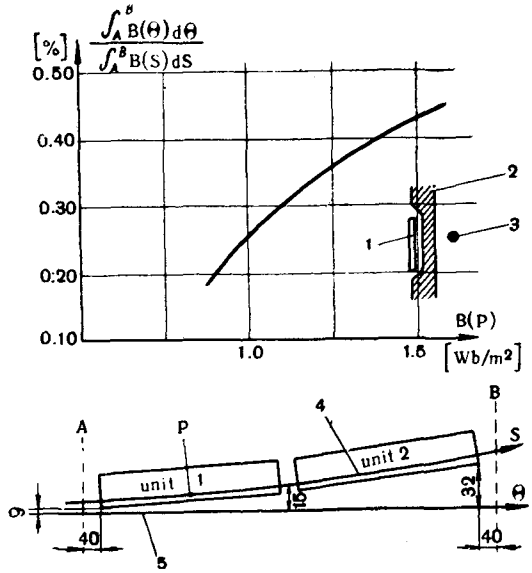

Fig. 18. Integrated leakage field as a function of the exitation level. Expressed as a percentage of the integrated bending magnet field:
1 — septum; *2* — shield; *3* — beam; *4* — $B\ (S)$ along trajectory in BM; *6* — $B\ (\theta)$ along equilibrium orbit CPS.

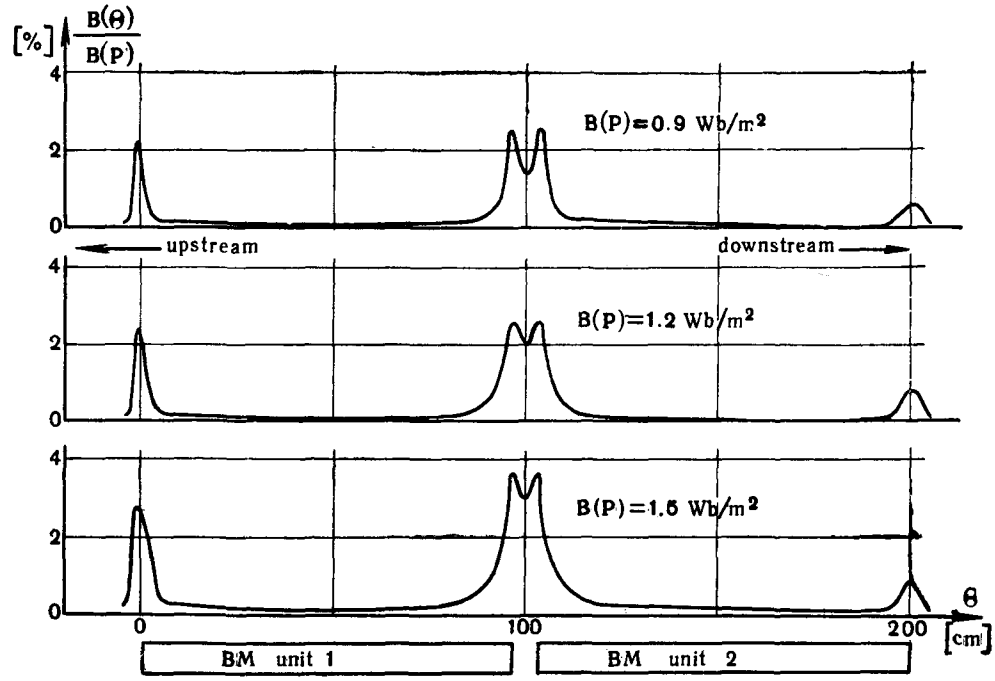

Fig. 17. Leakage field of the bending magnet as measured point to point along the undisturbed machine orbit (cp. the sketch of Fig. 18). Expressed as a percentage of the field $B\ (P)$ in the reference point P.

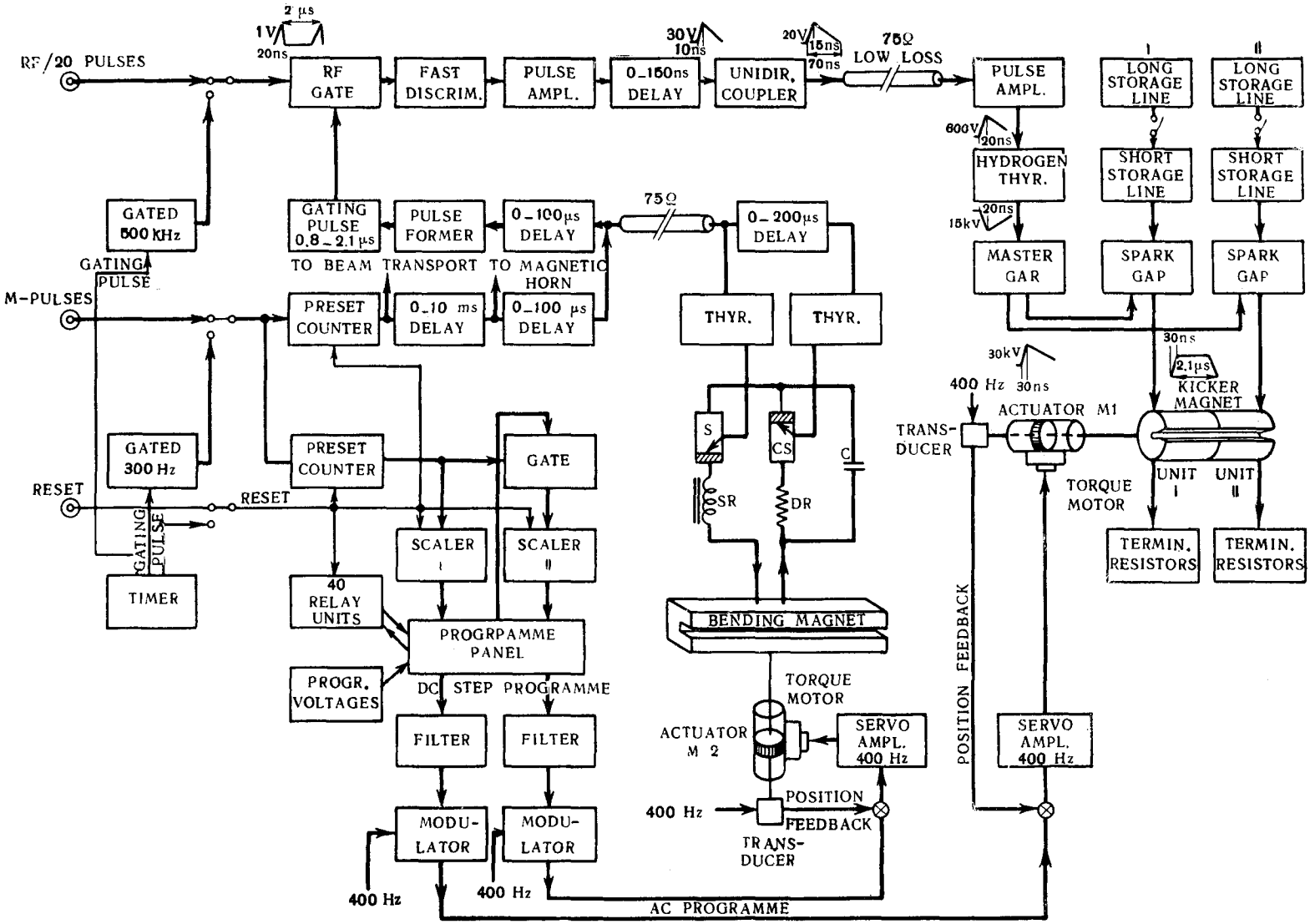

Fig. 19. Block diagram of the fast ejection controls.

tube scalers counting M-pulses. One scaler is gated via a relay unit from the other, thus permitting to delay the second programme to the first. The 100 taps of the stabilized dc voltage programme potentiometer, the contacts of twenty relay units, their coincidence connections and the scaler cathodes are united on a IBM programming panel on which the programmes can be composed.

Monitoring. The slow monitoring system using a double beam oscilloscope can at choice display the dc step programme, the modulated programme, and the principle feedbacks, representing movement, velocity and acceleration of the magnets, all either modulated or demodulated. A peak is permanently superimposed on the display at the moment of ejection. Finally, one channel displays the internal proton beam current in the synchrotron for observing possible interception if the magnet movement is adjusted. The fast monitoring system, using a Tektronix-585 scope, can display all signals pertaining to the magnets or the beam, such as the KM sparkgap triggering phenomenon, current pulse in kicker magnet and in bending magnet, magnetic field in the KM units, their sum, their difference (interlocked over a discriminator), the pulses arriving on the terminating resistors, BM and KM pulses superimposed (check on synchronisation), internal beam structure external beam structure, rise of kick and bunches superimposed.

The extracted beam can be observed on the screen of a television receiver with channels to different cameras. The first camera views the upstream end of the bending magnet bearing a fluorescent frame that covers the septum and the magnet around its aperture. Here one can see the bending magnet intercepting the beam and check whether the latter is kicked into the aperture. A second camera views a screen in straight section 2 on which the deflection of the bending magnet can be observed. The signal of the external beam structure comes an electrostatic pickup electrode around the beam after the screen in straight section 2. A beam current transformer with an integrator gives a digital display of the extracted number of protons and a totalizer gives the integral number. The position of the magnets at a given moment can be measured by making a zero setting between the 400 Hz position feedback signal from the servo-actuators and a 400 Hz voltage from a potentiometer. The zero indicator is gated at the desired moment.

7. SUPPORTING ENGINEERING

Considerable mechanical engineering effort was involved in manufacture and installation of the ejection equipment, besides for magnets and pulse generators mainly for the hydraulic movement and for the vacuum. Both actuators are three stage electro-hydraulical servo systems. The first stage is a torque motor driven by an electronic amplifier, the movement being fed back to the input of the amplifier by means of induction potentiometers. The kicker magnet and bending magnet have masses of about 250 and 450 kg, respectively. For displacement (acceleration and braking) over distances of 300 mm in times of the order of 100 ms they must have considerable thrust and will create corresponding reaction forces. They are therefore not supported on the concrete ring-shaped beam, bearing the CPS magnet, but their supporting girders are separately anchored into the concrete structure of the building. A hydraulic high pressure source with adequate power ratings is installed in the nearby sub-generator room. The oil is piped to the actuator over about 60 m distance. Each actuator is equipped with an input and output, oil accumulator which supplies respectively takes up the flow surges.

The vacuum tanks are basically aluminium boxes of adequate dimensions foreseen with enough easily removable covers to make the magnets accessible. The kicker magnet tank is equipped with one, the bending magnet tank with two type V3D Galileo diffusion pumps of capacity 3000 l/s, and each tank has a Heraeus type R-152 rootes pump, of capacity 150 m^3/h in parallel to reduce pump down time. The pump capacity has been overdimensioned on one hand for reasons of pump down time, on the other hand to have some margin for choosing materials for the ejection equipment that are less favourable for vacuum.

An interesting feature is the vacuum seal, around the actuator shaft of which a cut is shown in Fig. 20. The seal is mounted on the supporting girder of the actuator and connected with a bellows to the tank in order to avoid reaction forces on the latter. The two porous bronze rings align the seal around the shaft. For this purpose the inner seal has the necessary degrees of freedom. The seal has two stages with a pre-vacuum in between. The greasing is done with Apiezon C high vacuum oil, commonly used in diffusion pumps. The steel shaft is hard chromium plated and polished to a high gloss.

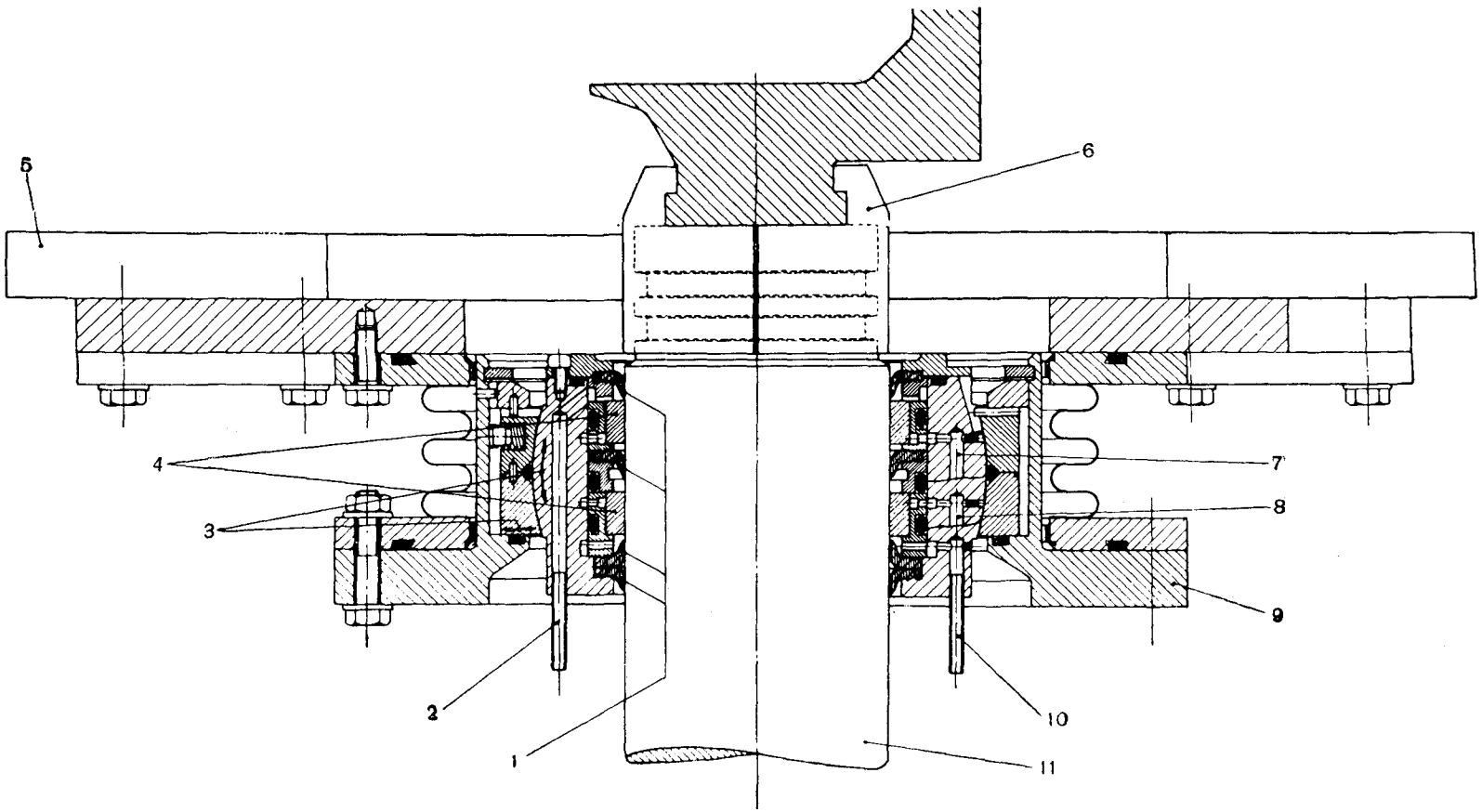

Fig. 20. Vacuum seals around the moving actuator shafts:

1 — neoprene sealing rings; *2* — rough vacuum; *3* — inner part of seal has 2 lateral degrees of freedom for translation and 3 for rotation; *4* — porous bronze rings guiding inner seal; *5* — bottom of vacuum tank in straight section 1; *6* — connection piece between shaft and bending magnet; *7* — greasing under vacuum; *8* — greasing under atmospheric pressure; *9* — outer casing of seal rigidly connected to actuator structure; *10* — leak oil recuperation; *11* — transmission shaft from actuator.

8. OPERATION AND EXPERIENCE

Apart from the accelerator as such and the ejection hardwere some facilities incorporated in the CPS are essential and some are convenient for operation of the extracted beam. The position of the closed orbit can be subject to some change in time. In order to avoid realigning of the ejection magnets, it is useful to have some simple means to adjust the beam position. For the kicker magnet this possibility is radially given by the movement itself, which can be adjusted to a large range of beam positions. In addition, so-called radial perturbations can be programmed and introduced as error signals in the phase of the beam control system, thus displacing the beam over a controlled radial distance at desired instances.

The beam can be locally displaced in the vertical direction by sets of two beam kickers, i. e. identical magnetic fields acting on the beam half a betatron wave length apart, thus creating a bump on the closed orbit. Two sets of these are available for ejection: one set making the bump in straight section 97, slightly affecting the vertical angle in straight section 1, and another for a bump in straight section 1. This possibility also exists radially. The halo of scattered protons around the beam, believed to be of the order of 0.1%, is prevented from hitting the ejection equipment by shaving it off. For this the beam is radially steered 2 cm inwards around 300 ms before ejection onto a target in straight section 12 that trims of the halo but does not affect the beam intensity. The radial perturbation is then suppressed and another one is introduced placing the beam at the right distance in front of the septum. This happens as shortly as possible before ejection but early enough to make a beam position reading. Several ms after ejection a strong inward perturbation dumps what remains of the internal beam onto the mentioned shaving target. The dumping operation is to avoid build-up of radioactivity in unwanted places in case anything is left circulating after ejection.

Some preliminaries precede the actual ejection [11]. They have been performed in early extraction experiments and are gradually being relaxed as more experience and confidence is fained. If the placing perturbation is increased until interception can be detected by loss of beam current and by light on the TV screen, then further until the total beam is lost, the radius of the beam is equal to the difference between the respective position readings. The reading at the onset of interception, corrected for the diameter, must corroborate with the supposed alignment of the bending magnet septum. One can now adjust a convenient clearing of 1 to 2 mm between the beam and the septum. The vertical position of the bending magnet at placing of the beam can be adjusted on the television screen. The light flash of beam interception should come from vertically, the centre of the septum.

The kicker magnet has its own additional razors (cp. Fig. 2) to protect it against the consequences of vertical beam disalignments. These razors consist of a fork at the downstream end of the magnet. The distance between the tips of the fork is 11 mm. This is 3 mm narrower than the other side, which follows the contours of the gap, but protrudes 0.5 mm into it. These razors trim the beam to its right vertical size as the magnet advances, leaving adequate clearings between beam and gap. The kicker magnet razors are used for check of the beam position to kicker magnet aperture. A reduced movement is set up, bringing the points of the fork over the beam. If no interception is observed this indicates a clearing of at least 1.5 mm between beam and magnet poles. Symmetry can be checked by creating bumps in the closed orbit until interception by upper or lower fork tip. The currents exciting these bumps must be equal and of opposite sign. This is so within the precision of the test. The kicker magnet stroke can then gradually be magnified until onset of beam interception by the magnet yoke. At this moment, the beam position reading, corrected for the diameter should corroborate with the magnet position as read on the comparator. Reducing the stroke, the kicker magnet is now placed in its working position, i. e. radially half way its aperture. If the kicker magnet is excited and the voltage is gradually being increased, one first sees on the television screen the beam falling on the septum and then it disappears into the aperture of the bending magnet. This can be checked by reducing the stroke of the BM, such that the kicked beam falls on the upper side of the frame.

The pulse shape (cp. Fig. 21) arising from unequal impedance of short storage line and long storage line makes that with small clearances and at the nominal voltage of 40 kV at 25 GeV on the kicker magnet pulser one extracts 18 bunches, i. e. only 90% of the beam, losing the first two on the bending magnet sep-

tum. By increasing the voltage to 45 kV 19 bunches are extracted (cp. Fig. 22) the missing second bunch corresponding to the dip in the pulse after the first peak. Replacing the short storage line by one having the right impedance, will bring the first peak up to the nominal value and the dip slightly below that level. 100% ejection, now only possible at higher voltages than commonly used in the first runs, will then become normal practice at presently used low voltages.

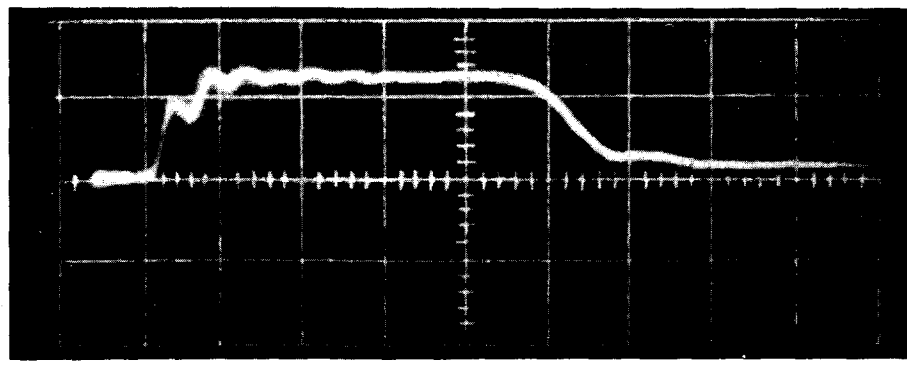

Fig. 21. Sum of the magnetic kicks in the two kicker magnet units. Each derived from a loop through the entire length of the unit. Sweep: 0.5 μs/div.

For this application one already has to synchronize the rise to the first peak between two subsequent proton bunches. Jitter and delay between the two pulsers has to be small. For diagnostical reasons this synchronization between bunches can best be done with single bunch ejection adjusting the delay in the fast channel until only one bunch disappears. Fis. 23 shows the internal beam structure after ejection of one bunch. The two mutilated bunches come from inflection and conveniently mark the revolution period. A typical particle trajectory, obtained by an electronic computer programme [12], is shown in Fig. 24. With the nominal current in the bending magnet the beam appears

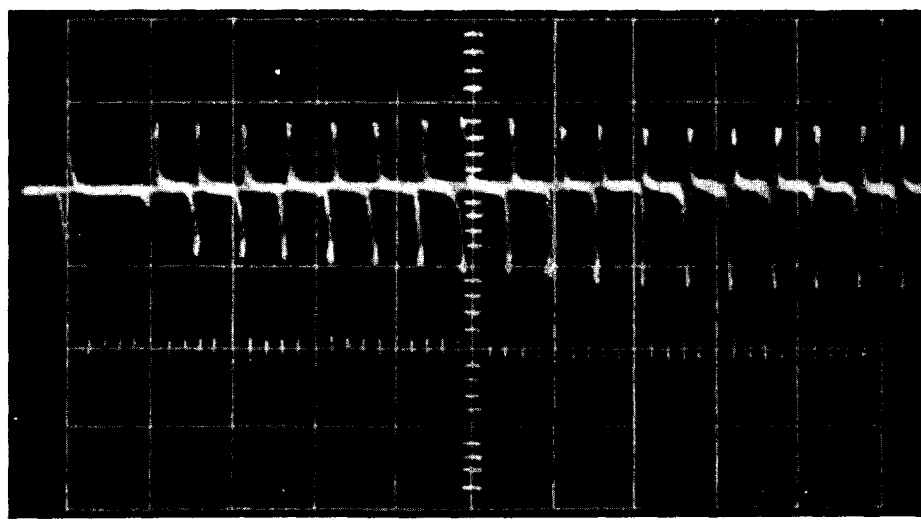

Fig. 22. Structure of the extracted beam. Second bunch lost on the septum due to dip in the kicker magnet field (cp. Fig. 21).

close to the calculated point on the screen of straight section 2, outside the CPS vacuum chamber. For the trajectory used in the CERN neutrino experiment [13] the computed phase ellips of the extracted beam in straight section 2 is compared to the internal emittance in Fig. 25. Finally, Fig. 26 is obtained from exposing photographic paper to a proton beam focu-

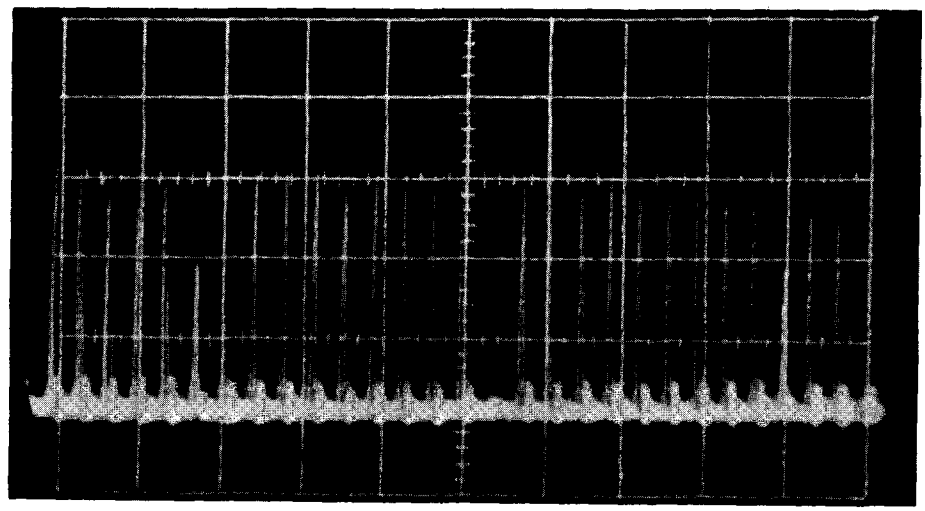

Fig. 23. Internal beam structure after the extraction of a single proton bunch. Distance between half peaks is one revolution. The half peak is the proton bunch mutilated at inflection.

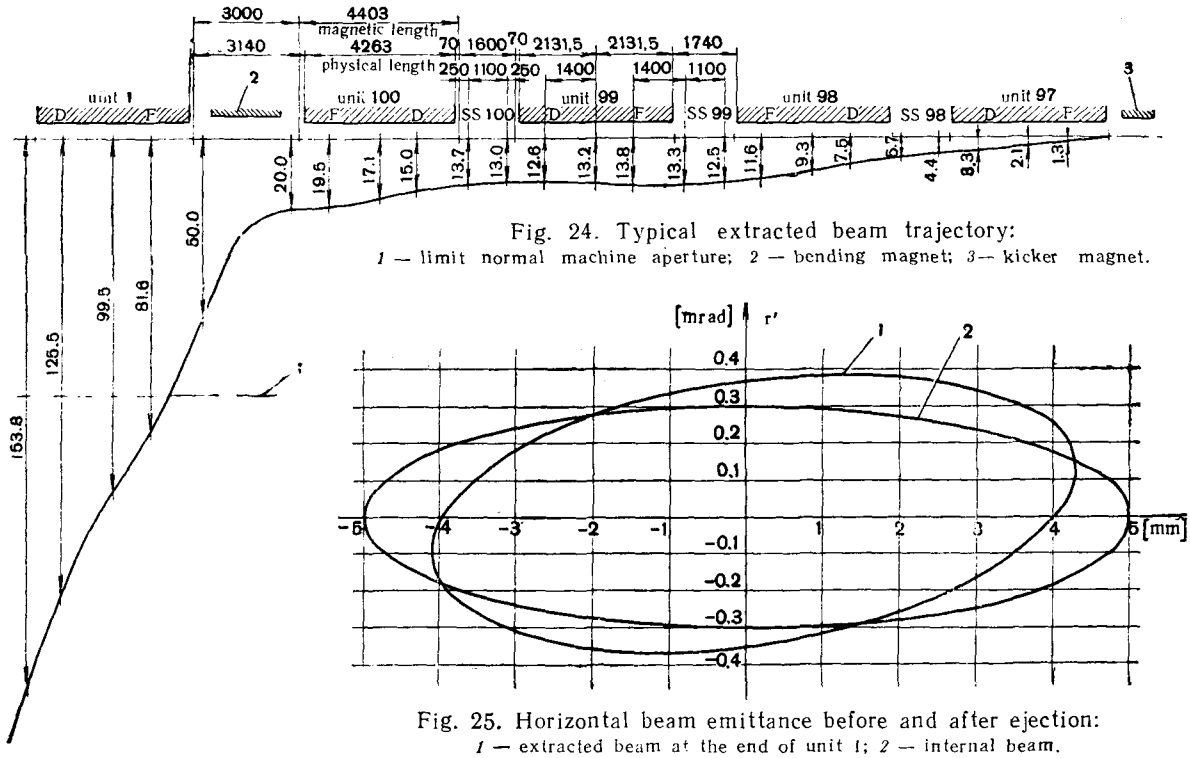

Fig. 24. Typical extracted beam trajectory:
1 — limit normal machine aperture; *2* — bending magnet; *3* — kicker magnet.

Fig. 25. Horizontal beam emittance before and after ejection:
1 — extracted beam at the end of unit 1; *2* — internal beam.

sed at the external target in the magnetic horn [13]. The fast ejection system has now completed several weeks of operation in the CERN neutrino experiment, to a total of

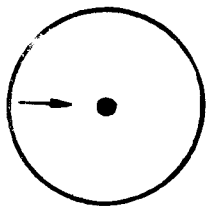

Fig. 26. Image spot of ejected beam, focused on an external target in the magnetic horn. True scale.

95% of its planned running time and with an average extracting efficiency of between 90 and 95%.

ACKNOWLEDGEMENT

Our thanks are in the first place due to the vacuum group under G. Munday for the substantial part they took in the project. It is a pleasure to thank here Mr. D. A. G. Neet who initiated design and construction of the controls. We are grateful to Dr. C. A. Ramm for his continuous support of the project, to Dr. H. G. Hereward for the patient way in which he coached us through the first ejection sessions with the CPS, and to the machine engineers and operators for their constant friendly collaboration. Finally, without the active and intelligent help of our CERN mechanics this job would not have been done.

REFERENCES

1. Citron A. On a possible ejection scheme. CERN PS/AC-5, July 1954.
2. Kuiper B. and Plass G. On the fast extraction of particles from a 25 GeV synchrotron. CERN 59-30, Aug. 24, 1959.
3. Krienen F. Report on slow ejection system 25 GeV protonsynchrotron. CERN 59-21, March 14, 1959.
4. Hereward H. G. The possibility of resonant extraction from the CPS. CERN AR/Int. GS/61-5, Dec. 7, 1961.
5. Regenstreif E. The CERN proton synchrotron: 1st part — CERN 59-29, Aug. 21, 1959; 2nd part — CERN 60-26, July 29, 1960; 3rd part — CERN 62-3, Jan. 8, 1962.
6. O'Neill G. K. and Korenman V. The delay line inflector. Princeton Pennsylvania Accelerator Project, GKON-10, VK-13, Dec. 18, 1957.
7. O'Neill G. K. Storage rings for electrons and protons. In: Proceedings of the International Conference on High Energy Accelerators and Instrumentation (CERN, 1959).
8. Falnes J. Loaded transmission lines as inflectors for the storage ring. CERN AR/Int. SR/61-8, March 13, 1961.
9. Fitch R. A. and McCormick N. R. Low inductance switching using parallel spark gaps. I.E.E. Convention on thermonuclear processes, Apr. 1959.
10. Neet D. A. G. Proposed electronic controls for the south hall fast ejection system of the proton synchrotron. CERN NPA/Int. 61-19, Aug. 23, 1961.
11. Hereward H. G., Kuiper B., Plass G. Setting up the fast ejected beam. CERN NPA/E GP/fv, Apr. 8, 1963.
12. Kuiper B., Lake D., Plass G. Computation of trajectories in the CPS magnet field with a mercury programme. CERN PS/Int. EA 59-14, Dec. 7, 1959.
13. Giesch M. et al. Status of magnetic horn and neutrino beam. In: Proceedings of the Conference on Instrumentation for High Energy Physics, 1962; J. Nucl. Instrum. and Methods, 20, 58 (1963).